Application of Motion Capture Attributes to Individual Identification under Corridor Surveillance

A. MIHÁLIK, R. ĎURIKOVIČ AND M. SEJČ

Abstract

Accurate and fast identification of a person from a security point of view is a key procedure. The most common technique of person identification uses identity cards. In contrary to the common approach we focus our research on identification based on the body movement such as the gait in this paper. The gait and the posture belong to the unique characteristics of the person that helps us to facilitate the identification. The proposed methodology allows us to incorporate personal characteristics into the access control systems using the color depth camera (RGBD). For the sake of gait analysis, the important task is to recognize the figure and extract the skeleton data from a video recording. Besides the usage of the mathematical statistics methods, we are opting to use computer animation and computer vision methods, which makes the research interdisciplinary. The main novelty of the paper is the definition and extraction of the feature vector from motion capture data, the analysis methodology and finally the selection of few statistically dominant motion attributes for the identification purposes. Besides the development of new approaches in this field, we validate proposed approaches from the perspective of accuracy.

Mathematics Subject Classification 2000: 94A08, 68U10, 68P01, 68U05
Keywords: Motion identification, Security, Feature vector, Mocap data

1. INTRODUCTION

The right and fast identification of people from a security point of view is a key procedure, in today's world. Each person is unique. The most common way of identifying a person is based on identity cards. In a worse case, only the password or pin use is sufficient. Such identity keys can be easily stolen or falsified. It is, therefore, necessary to focus on the unique qualities of every person that cannot be imitated, lost or forgotten.

Biometrics authentication refers to the identification based on the unique features of a particular person. We can categorize biometric identifiers into two separate groups; either the physiological or the behavioral characteristics. Physiological characteristics are related to the body and its shape or structure such as fingerprint [Wang et al. 2010] or DNA [Tautz 1989]. Behavioral characteristics are related to the pattern of behavior of a person such as voice, handwriting or leg motion [Yam et al. 2002].

A person's walk is unique, as confirmed by an experiment [Barclay et al. 1978]

10.2478/jamsi-2018-0004

DE GRUYTER OPEN

that was carried out in the 1970s. However, as has been shown later, a person can be identified with much greater accuracy based on the use of selected symptoms. The survey [Gianaria et al. 2014] showed that it is possible to achieve up to 96% success. In particular, they used fixed human skeleton parameters such as the height of the person or the length of the limbs. In our method, we will use some of their verified attributes. However, our project focuses mainly on walking. To analyze a walking cycle statistical methods are commonly utilized. Some approaches are based on feature learning methods for gait recognition [Feng et al. 2016], others use probabilistic methods [Bazin and Nixon 2005]. On the other hand, descriptors describing actual behavior of individuals have already been studied. In particular, there are descriptors aimed at detecting aggressive behavior [Chen et al. 2008] or detecting human action [Acar et al. 2012]. These methods share a common key feature. They try to describe all people as a group and are therefore not suitable for distinguishing individuals.

A crucial step in analyzing the walking sequence is data acquisition. In our case, it will be the captured animation of a human skeleton. Our approach to quickly extract skeleton and human movement based on depth data rely on freely available software development kit (SDK) for Kinect device [Rahman and Gavrilova 2017; Peterkova and Stremy 2015]. However, the SDK is well known for its inaccuracy. Another choice is extracting the skeleton from depth data using an anatomical human model [Zhu et al. 2015]. The skeleton thus obtained is very precise compared to the previous option, but it is paid off by a calculation time that is too large for the practical real-time application, particularly for several people at the same time. An alternative is the use of color video information [Andriluka et al. 2009]. Color-based methods are difficult to calibrate and apply in practice under unstable light conditions. Therefore, we propose a combination of color and depth information [Dubois and Bresciani 2015] that will enable us to take advantage of both approaches.

The process of the identification comprises of particular steps devoted to the feature extraction and the database of subjects search procedure. First, the multiple subjects during the gait had to be recorded. Then the skeletal representation of the data is extracted using the particular procedure [Riečický et al. 2018; Ďurikovič and Madaras 2015]. The feature vector is created from the data of each subject and subsequently stored in the database. The main focus of our work is to find the relevant parameters to construct the feature vector using in the database.

2. SKELETON MODEL

To capture the behavioral characteristics of gait we based our data structure on physiological characteristics of human skeleton depicted in Fig. 1. Our designed hierarchical data structure is meant to be compatible with Biovision Hierarchy (BVH) data format. BVH format is commonly used in many animation systems and software platforms. The proposed skeletal structure is extracted from the sequences capturing human actors walking data [Kim and Kim 2014]. We extract the 3D position of joints, representing nodes in the hierarchical structure, from default posture. The structure contains 5 leaf nodes and the root of the structure is the node in 3D space denoted as P_1. We can represent walking animation as a sequence of poses attribute to subsequent time frames. Each joint can rotate about preceding node, therefore we can create an arbitrary pose from default posture using a particular set of rotations. If we rotate root, we rotate the whole skeleton. If we rotate shoulder joint, the whole hand is moved. Therefore, we can represent skeleton in each animation frame using our hierarchical representation. The optimal number of frames per second (fps) capturing walking cycle of regular gait is 30, see Fig. 1. To capture the running person we need at least 60 fps to achieve smooth motion.

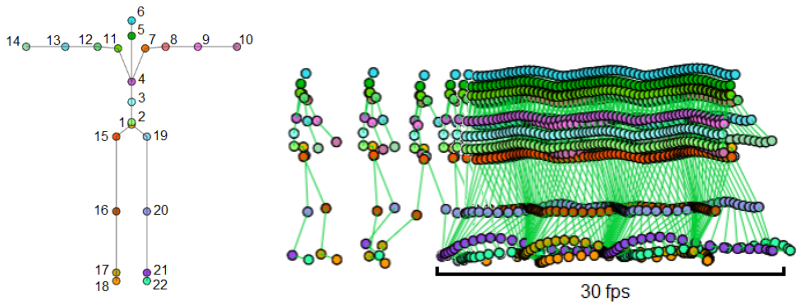

Fig. 1. Model of skeleton. Left: Joints P_1-loins (center), P_2-rump, P_3-lower back, P_4-upper back, P_5-neck, P_6-head, P_7-left arm, P_8-left hand, P_9-left elbow, P_{10}-left palm, P_{11}-right arm, P_{12}-right hand, P_{13}-right elbow, P_{14}-right palm, P_{15}-right hip joint, P_{16}-right knee, P_{17}-right heel, P_{18}-right tiptoe, P_{19}-left hip joint, P_{20}-left knee, P_{21}-left heel, P_{22}-left tiptoe. Right: Walking frame sequence.

3. GAIT ATTRIBUTES

We consider three particular parameter categories in order to analyze gait. Physiological, kinematic and time-dependent parameters. We have analyzed each group of parameters in order to find appropriate parameters suitable to form a feature vector. As an example of physiological parameter we can use the length of a limb or the height of a person which is a scalar value. The kinematic parameter is, for example, the pace, which could change during the walk. The time-dependent parameter is, for example, arm rotation, which could be different in each frame.

3.1. Physiological parameters

Physiological parameters of the same person are constant at each time of movement. They can be calculated from one arbitrary frame. In our method, we used 5 physiological parameters. These include the height of the torso, left and right-hand lengths, left and right leg lengths. When evaluating these parameters, the distance between the joints is calculated. Each of the joints is represented as a point P in a three-dimensional space. So the distance between the two joints is calculated as the Euclidean distance of two points. The resulting value will be the sum of the distances between every two adjacent joints of the sequence. Parameters representing the lengths of particular body part L_w are calculated using the formula:

$$L_w = \sum_{i \in w} \| P_{w_{i+1}} - P_{w_i} \|, \tag{1}$$

where w represents a set of joints from a given limb (see Fig. 1). The indexes of the joints from these sets are found in the Tab. I. We have calculated these distances for each frame separately. The resulting value was the average of the values from all frames to minimize minor inaccuracies.

Table I. Joints sequences. Symbol of the parameter its explanation and the corresponding sequence of joints for calculation.

Symbol	Parameter	w
γ	Torso height	$\{6, 5, 4, 3, 2, 1\}$
α_P	Right hand length	$\{12, 13, 14\}$
α_L	Length of left hand	$\{8, 9, 10\}$
β_P	Right leg length	$\{15, 16, 17\}$
β_L	Length of left foot	$\{19, 20, 21\}$

3.2. Kinematic parameters

Kinematic parameters include attributes that can be changed at each step of the walk. These include, for example, walking speed, step length, etc. Altogether, we investigated up to 30 parameters that could be relevant to the identification. However, it turned out that most of them depend on the spatial position of the skeleton. Therefore, we have excluded such parameters. Finally, we have 10 parameters that we have further analyzed. The parameter list is listed in the Tab. II.

Table II. List of kinematic parameters with parameter notation and the explanation.

Parameter	Description
υ	Speed
δ_L	Step length of left leg
δ_P	Step length of right leg
κ	Step width
$\sigma^2_{P_6,x}$	Variance of head on x axis
$\sigma^2_{P_6,y}$	Variance of head on y axis
$\sigma^2_{P_{20},y}$	Variance of left knee on y axis
$\sigma^2_{P_{16},y}$	Variance of right knee on y axis
$\sigma^2_{P_7,x}$	Variance of left arm on x axis
$\sigma^2_{P_{11},x}$	Variance of right arm on x axis

Kinematic parameters are not constant as physiological parameters. For one person, they can change at each step. To calculate them, we will need several frames capturing at least 2 steps gait cycle from the whole walk. The gait cycle means that the left and right legs touch the ground twice so that the length of the step can be calculated. The number of frames captured during the gait cycle cannot be uniquely determined. It depends on the number of frames per second and the speed of the recorded walk.

3.3. Walking speed

Walking speed is a numeric value indicating the length of the path per time interval. Specifically, the distance that the point P_1 (see Fig. 1) passes. However, we need to choose a suitable time step. Because the input data contains an integer number of fps (30, 60, ...), one second was the most appropriate choice.

Input data we have contains 30 fps, but it does not have to be the rule. Thus we select every thirty-one frame from the whole walk sequence. From each of the two selected consecutive frames, we calculated what distance point P_1 passes. These distances indicate the length of the path the person underwent for each second of the walk. Even

though the walking speed should be theoretically constant, not all of these values are the same. In the same second, the observed person can slightly accelerate or slow down. We have attempted to use the arithmetic mean of this data, which has proven to be an incorrect choice. In some cases, the tracking person started to slow down at the end of the walk, causing the results to be distorted. Finally, we determine the resulting velocity as the median of the obtained data.

3.4. Step length

In our experiments, we use two parameters for step length. One for the left and the other for the right leg. It turns out that one does not have to do the same long steps for each of the lower limbs. The length of the step was counted as the distance of two points in which the foot of the same leg touched the ground. These points are shown in the Fig. 2. The image shows the touch of the left foot to the floor.

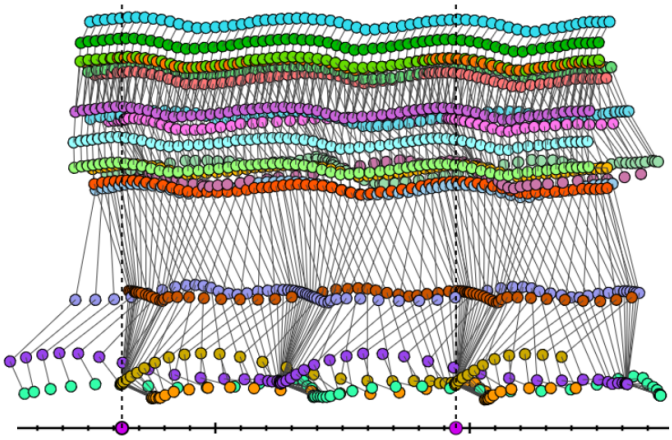

Fig. 2. Step length of left leg. X-axis shows the step start and the end.

To calculate the distance we first need to detect the positions where the foot touched the ground. However, the floor was not defined. It could be at any height relative to the coordinate system. Using height coordinates to detect contact with the floor was not possible.

During walking legs are alternating. For example, the right foot moves while the left is standing in place and does not change its position. The left foot will move only when we are touching the floor with the right foot. So at the moment of touching the

floor, the foot position does not change. This means that the position of the foot is the same in several consecutive frames. From the Fig. 2 we can see that the density of the points representing the heel is higher in this particular location.

The positions where the density was the highest are exactly the points where the foot touched the floor. In this way, we received several consecutive points representing the touch with the floor. Finally, we calculate the distances between consecutive touch points representing the particular step length. However, we always needed a sequence of walks in which the person would have done at least two steps. For the same person, the length of the steps during the whole walk could be slightly different. We obtain the resulting value as the median of the calculated data. Along the whole walking sequence, we captured variable step lengths and create the list of step lengths. As a resulting length, we choose median computed from the list of captured lengths. However, it is true that the longer the record of the walk, the more accurate the results are.

3.5. Step width

This parameter determines what the distance between each heel is. To calculate this value, we need to detect where the feet touch the ground. Acquired points are projected onto the floor represented by the XZ plane. Therefore, we can consider these points as 2D, shown in the Fig. 3 and indexed from 1 to 5.

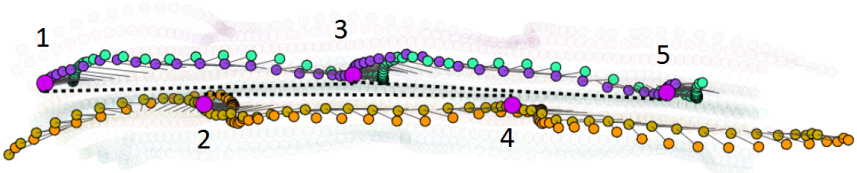

Fig. 3. Step width - top view. Dots show the left and the right leg movements, the distance between parallel dot lines can proximate the width of a step in that location.

We have found a linear regression for three consecutive points corresponding to left and right leg, respectively. Two lines we found are sketched in the Fig. 3 with a dashed line. We then calculate the distances of the line $(1,3,5)$ from the center of the line $(2,4)$. In this way, we also obtained variance data caused by the person being occasionally directed to the sides during the movement. These occasional extremes

could cause a significant amount of distortion when averaging the values, so we again used the median of the data.

3.6. Variance of head, knee and arm

Variance gives us the size of the range in which the observed values are found. It is denoted as σ^2 and can be calculated using the formula:

$$\sigma^2 = \frac{1}{N-1}\sum_{i=1}^{N}(x_i - \mu)^2, \tag{2}$$

where N is the number of samples and μ is the mean value. In Fig. 4 we can see the top view of the walking person. Particular points represent the movement of the head along the Z axis. The solid line, denoted as μ, represents the mean value. Variable σ^2 is represented by a dotted line and represents the range at which the points are distributed.

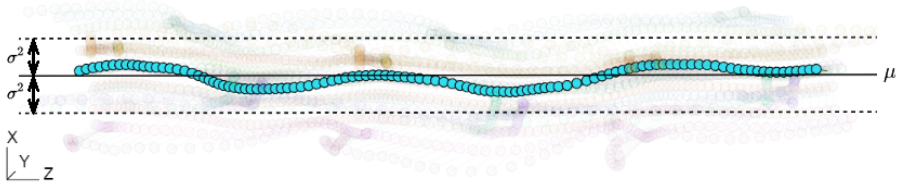

Fig. 4. Variance of head movement. Middle line is the mean value μ of head position, the dots show the head movement and σ^2 is the variance.

This approach is valid only if the monitored person always walks in the direction of the Z axis. For arbitrary direction, we use the linear regression instead of the mean value (see Fig. 5). Let us consider a line $\hat{y}$ that approximates particular points much better than average μ. Using this line we are able to calculate the size of the mean quadratic deviation MSE:

$$MSE = \frac{\sum_{i=1}^{N}(y_i - \hat{y}_i)^2}{N-2}, \tag{3}$$

where N is the number of points, y_i is y coordinate of the i-th point and $\hat{y}_i$ is the mean value at point i calculated as line $\hat{y}_i = \beta_0 + \beta_1 x_i$. β_0 and β_1 are coefficients obtained by linear regression. The variance of knee and arm is estimated same way tracking particular joints instead of the head.

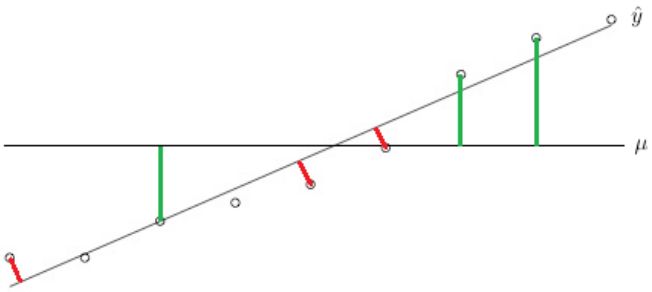

Fig. 5. Linear regression $\hat{y}$ and mean value μ.

4. ANALYSIS OF PHYSIOLOGICAL AND KINEMATIC PARAMETERS

Firstly, we have focused to find the similarities in the multiple records of the walking sequence recording same person. We have searched for the scalar values similar to multiple recordings of the same person. PCA can be utilized to find relevant axes in multidimensional space. We have multidimensional space of multiple parameters. PCA is used to find the direction of maximal variance in physiological and kinematic parameters multidimensional space. The most relevant parameters have its axes oriented in the direction of maximal variance.

5. TIME DEPENDENT PARAMETERS

In this section, we describe parameters that are time dependent. It will no longer be a one-dimensional value, as it was with physiological or kinematic parameters, but a sequence of values depending on time. We may find many parameters that vary with time. However, we decided to investigate joint acceleration, arm rotation, bending and leg distances. A complete overview of the parameters is described in Tab. III.

5.1. Acceleration

We have examined the acceleration of the various joints over time. The result was a signal that shows the magnitude of the acceleration as a function of time. The resulting acceleration values a are calculated using the formula:

$$a = \frac{v_2 - v_1}{t_2 - t_1}. \tag{4}$$

Table III. List of time dependent parameters. Parameter corresponding to relevant joints and their explanation.

Parameter	Description	Parameter	Description
a_{P_6}	head acceleration	ω_v	vertical rotation of arm
a_{P_1}	hip acceleration	ω_h	horizontal rotation of arm
a_{P_9}	left knee acceleration	$d_{P_{10,14}}$	palms distance
$a_{P_{13}}$	left elbow acceleration	$d_{P_{9,13}}$	elbows distance
$a_{P_{10}}$	left palm acceleration	$d_{P_{16,20}}$	knees distance
$a_{P_{14}}$	right palm acceleration	$d_{P_{17,21}}$	heels distance
$a_{P_{20}}$	left knee acceleration	$d_{P_{18,22}}$	tiptoes distance
$a_{P_{16}}$	right knee acceleration	φ_n	tilt of the head
$a_{P_{21}}$	left heel acceleration	φ_γ	tilt of the torso
$a_{P_{17}}$	right heel acceleration	φ_{α_L}	left arm bending
$a_{P_{22}}$	left tiptoe acceleration	φ_{α_P}	right arm bending
$a_{P_{18}}$	right tiptoe acceleration	φ_{β_L}	left leg bending
		φ_{β_P}	right leg bending

To calculate acceleration, we need to know the speeds of v_1 and v_2, that can be calculated using the formula:

$$v = \frac{\|P_2 - P_1\|}{t_2 - t_1}, \tag{5}$$

where P_1 and P_2 are points representing joint positions at t_1 and t_2, v_1 and v_2 are speeds in time t_1 and t_2, respectively.

This way we calculated the magnitudes of acceleration over time. We plotted the resulting values in a graph where axis x represents time and axis y acceleration, depicted in Fig. 6.

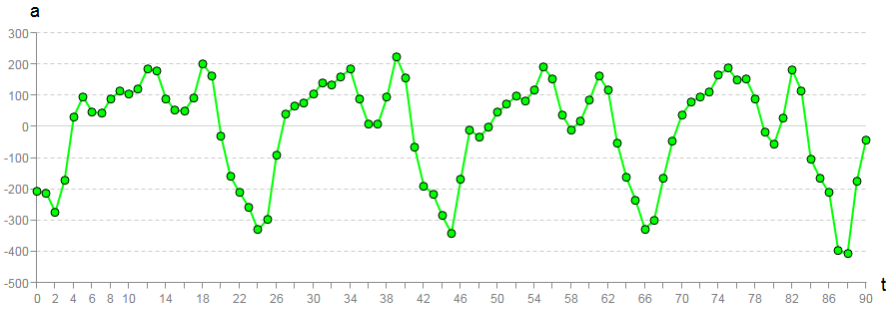

Fig. 6. Hip joint acceleration.

As we can see from the figure, the signal is not smooth but it is slightly shaken.

This is because footage consists of only 30 frames per second. If we had a record of walking with more robust sampling, the signal would be smoother. We used the triangle smoothing function [O'haver 2016], that uses the weighted average of the ambient values for signal smoothing. These values were calculated using the formula in Eq. 6.

$$X_i = \frac{Y_{i-2} + 2Y_{i-1} + 3Y_i + 2Y_{i+1} + Y_{i+2}}{9}, \tag{6}$$

where Y represents the input and X output signal. After using the smoothing function, we received a signal that can be seen in the Fig. 7.

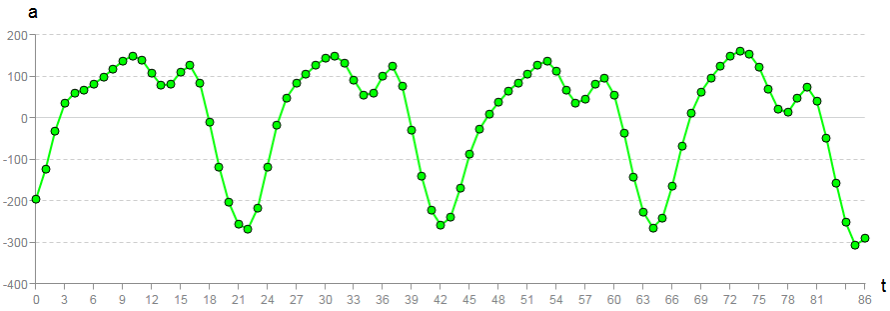

Fig. 7. Hip joint acceleration - smoothed signal.

5.2. Arms rotation

Another parameter we studied was the rotation of the arms. Walking person usually moves his shoulders. One shoulder moves upwards, while the other downwards. Concurrently, one moves forward and the other moves backwards. These are the two basic moves we perform with our shoulders as we walk. If we imagine a straight line passing through both arms, it would change its angle with respect to the floor and also to any vertical plane. That is why we call these movements as horizontal and vertical rotation of the arms, respectively. The illustration of the moves can be seen in the Fig. 8.

We use P_8 and P_{12}, see Fig. 1 and calculate the directional vector:

$$\vec{v} = \left(P_{12,x} - P_{8,x},\ P_{12,y} - P_{8,y},\ P_{12,z} - P_{8,z}\right), \tag{7}$$

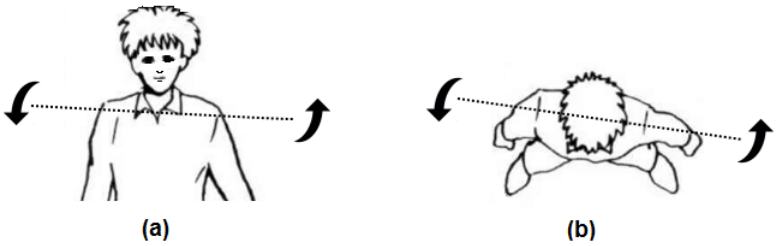

Fig. 8. Horizontal (a) a vertical (b) arms rotation.

where $P_{i,x}$, $P_{i,y}$ and $P_{i,z}$ represent the coordinates x, y, z of P_i, $i \in \{12, 8\}$. Subsequently, we calculated cosine of angle between vector $\vec{v}$ and the horizontal plane (Eq. 8) and the cosine angle between vector $\vec{v}$ and the vertical plane (Eq. 9).

$$\omega_h = |\vec{n_h}| \cdot |\vec{v}|, \tag{8}$$

$$\omega_v = |\vec{n_v}| \cdot |\vec{v}|, \tag{9}$$

where vector $\vec{n_h}$ was a normal vector of floor (0, 1, 0). For vertical rotation, vector $\vec{n_v}$ represented the normal vector of the plane YX, i.e. (0, 0, 1). Change of the cosine angles between individual frames plot to a graph, which can be seen in the Fig.9. The signal is also smoothed by the triangle smoothing function.

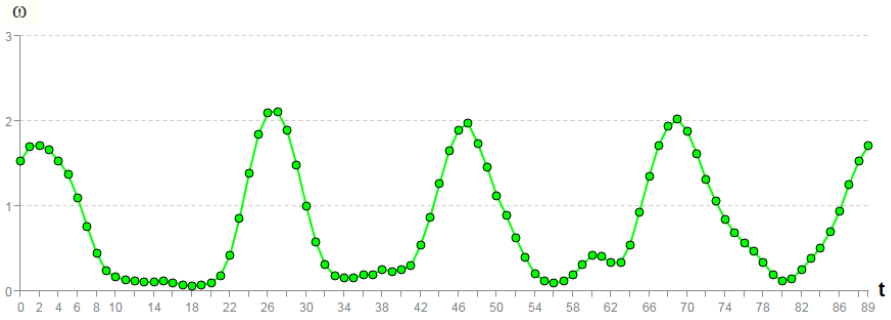

Fig. 9. Magnitude of vertical rotation of arms.

5.3. Distances

If we observe walking person, we may notice that the distance from the left palm to the right one is changing. We have decided to examine whether this change in the distance could be a characteristic feature for someone. During the investigation, we also focused on changing the elbows, knees and foot's distance. In addition, we studied the heel and tiptoe of the foot. So, overall, we have got up to 5 parameters.

Individual joints are defined as points in space and the Euclidean distance is calculated for the given joints in each frame. We plot the resulting values in the graph with the corresponding frame time, see Fig. 10. Where the axis y represents the distance value and the axis x is time expressed by the number of frames. There was almost no noise in this signal and it was not necessary to filter it.

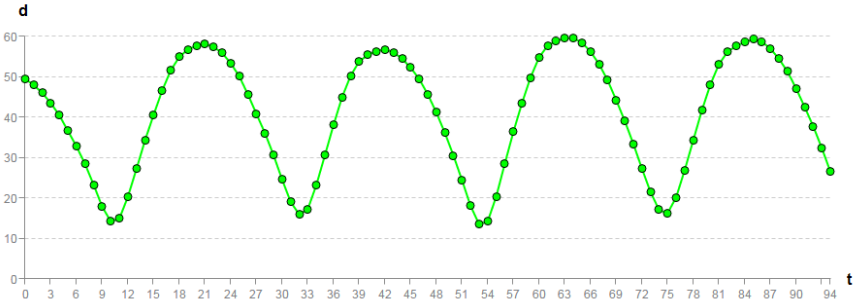

Fig. 10. Heels distance

5.4. Tilt and bending

Next we analyze the attributes such as a bending of an arm, a leg, a tilting of the neck and the whole body.

The hand and the leg have three joints in our case. Let us denote these joins as A, B and C, see Fig. 11. The resulting bend was calculated as the ratio of the length of the limb to the distance between the points A and C. For example, the right leg bending was calculated using Eq. 10.

$$\varphi_{\beta_P} = \frac{\beta_P}{\|P_{15} - P_{17}\|}, \tag{10}$$

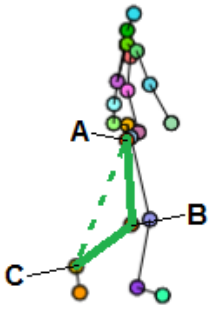

Fig. 11. Leg bending.

where β_P is the length of the right leg. We applied this calculation to each slide. The result is a graph that can be seen in Fig. 12, where axis y represents the ratio of the distances φ_{β_P} and axis x time by the number of frames.

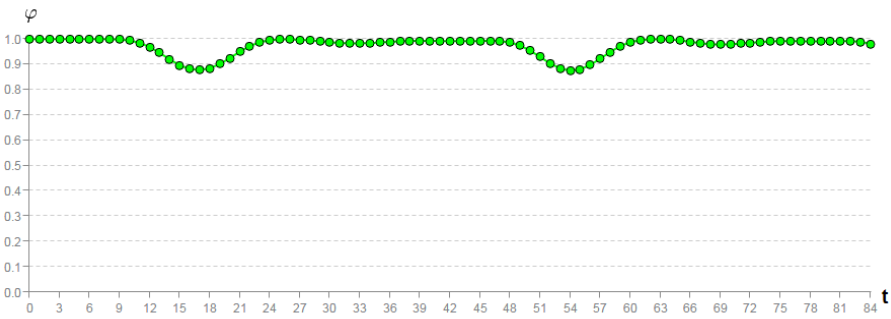

Fig. 12. Right leg bending.

The tilt of the whole body was calculated as the distance of the vertical line passing through point P_1 from point P_6, see Fig. 1. This way we found the movement of the head in relation to the center of body. The resulting graph, however, rather resembled

a mixture of random values than the periodic signal. For this reason, we consider the signal irrelevant.

6. ANALYSIS OF TIME DEPENDENT PARAMETER

When analyzing time-dependent parameters, we have 10 records of the same person. From each record, we calculate all 25 parameters listed on the Tab. III. The purpose of the analysis was to find out which of these parameters could be used to uniquely identify a person.

We compared each parameter using the cross correlation of two signals [Telford et al. 1990]. We were able to calculate the match between the two signals. The match can be expressed by a numerical value in the range $\langle$-1,1$\rangle$, where 1 represents a 100% match.

Consequently, we were able to create a 10×10 matrix for each of the parameters, where we compared every record with each other based on a specific parameter. Each of these matrices was symmetric because the match between record 1 and record 2 must be the same as the match between record 2 and record 1. The diagonal was always 1 because it was a comparison of two identical records. Overall, we have received 25 matrices and our goal was to find those where the diagonal elements were as close as possible to 1. For this purpose, we used multidimensional scaling [Borg and Groenen 2013] method (MDS) to help us select these matrices.

From our input matrices, however, we needed to choose those with the lowest scatter of data. This meant that the size of the resulting dimension should be small. Using the MDS we can compute a matrix containing the coordinates of the points in the new space. The smaller the size, the parameter was more relevant. Based on the calculated eigenvalues, we can sort input parameters. The first eigenvalue was always the largest and it was the dominant axis of the new space. The Tab. IV contains the parameters sorted according to the eigenvalues from the smallest to the largest.

Based on this analysis, we were able to select parameters that are the most similar to records of one person. We chose to select those whose value is $e_1 < 0.1$. Consequently, we needed to find out which of these parameters are different for different people. The procedure was the same as in the previous case, with the difference that we used 8 records from 8 different people. In this case, however, we were looking for parameters whose value e_1 would be as large as possible to determine which parameters differentiate people. The results of the above analysis are written in the Tab. V.

Table IV. Time dependent parameters. Parameter notation, the parameter explanation and the relevant eigenvalue.

	Parameter	Description	e_1
1	$a_{P_{20}}$	left knee acceleration	0.0586
2	φ_{β_P}	bending of right leg	0.0600
3	$d_{P_{18,22}}$	distance of tiptoes	0.0617
4	$a_{P_{22}}$	acceleration of left tiptoe	0.0651
5	$d_{P_{17,21}}$	heels distance	0.0658
6	$a_{P_{17}}$	right heel acceleration	0.0706
7	$a_{P_{18}}$	right tiptoe acceleration	0.0733
8	φ_{β_L}	left leg bending	0.0805
9	$d_{P_{16,20}}$	knees distance	0.0831
10	$a_{P_{21}}$	left heel acceleration	0.0836
11	a_{P_1}	hips acceleration	0.1077
12	a_{P_6}	head acceleration	0.1114
13	$a_{P_{13}}$	right elbow acceleration	0.1147
14	$a_{P_{16}}$	right knee acceleration	0.1156
15	a_{P_9}	left elbow acceleration	0.1385
16	$a_{P_{14}}$	right palm acceleration	0.1399
17	$a_{P_{10}}$	left palm acceleration	0.1426
18	$d_{P_{9,13}}$	elbows distance	0.1809
19	φ_γ	tilt of torso	0.2010
20	$d_{P_{10,14}}$	palms distance	0.2036
21	φ_{α_P}	bending of right arm	0.3648
22	ω_h	horizontal arm rotation	0.3923
23	φ_{α_L}	bending of left arm	0.3935
24	ω_v	arm rotation vertical	0.4794
25	φ_n	tilt of the head	0.5272

Table V. Sorted time-dependent parameters that are different for different people. Parameter notation, the parameter explanation and the relevant eigenvalue.

	Parameter	Description	e_1
1	$d_{P_{17,21}}$	heels distance	0.4325
2	$d_{P_{16,20}}$	knees distance	0.4000
3	$a_{P_{17}}$	right heel acceleration	0.2251
4	$a_{P_{21}}$	left heel acceleration	0.2124
5	φ_{β_L}	bending of left leg	0.2119
6	φ_{β_P}	bending of right leg	0.1597
7	$a_{P_{20}}$	left knee acceleration	0.1273
8	$d_{P_{18,22}}$	tiptoes distance	-
9	$a_{P_{22}}$	left tiptoe acceleration	-
10	$a_{P_{18}}$	right tiptoe acceleration	-

7. CONCLUSIONS

Novelty of our work is in the determination of parameter that most relevantly describes the individual in the context of gait. We have 32 records capturing gait of 8 different people. From the original 32 records, 11 of them were stored in the database. Each person had at least one record. Our goal was to assign the remaining 21 records to the right person.

During testing, we relied on data obtained from the analysis. We tested whether we can uniquely assign the gait to the right person. We tested various combinations of parameters. The results of the comparison are listed the Tab. VI. In addition to the selection of parameters, we also changed their weights in the test. We tried to give more weight to the more relevant parameter than the less relevant. Weight was a real number that multiplied the strength of each parameter. Parameters that were not listed in the table had a weight set to 0. It has turned out, that even for the parameters that have been identified as least relevant (e.g. arm rotation), we have managed to correctly assign up to 62% of walking records. This meant that each parameter, regardless of its relevance, uniquely describes the gait of person. In addition, further research has shown that different group of parameters is able to describe each group of people differently. For example, for individuals 1-4, some parameters have greater significance than for people 5-8. For another set of parameters, this was the opposite. This means that each person performs one of the movements of the limbs in a unique way that is specific to that person only. For each person, however, this limb or joint is different. This makes it very difficult to find a universal parameter that would identify the person with a 100% success rate. Success rate indicates how two particular feature vectors are similar to each other. For example, 100% success rate says, that the feature vector obtained during the gait analysis of investigated person is exactly same as a particular vector in the database of recorded subjects and therefore it is expected, that the person is identical. However, the key to clear identification may lie in the possible combinations of parameters, which would be perfectly balanced.

Table VI. Result validation. List of nonzero parameter weights used in identification process and the corresponding success rate.

Parameter weights	Success rate
$V(\gamma)=1, V(\alpha_P)=1, V(\alpha_L)=1, V(\beta_P)=1, V(\beta_L)=1$	100%
$V(\gamma)=3, V(\alpha_P)=3, V(\alpha_L)=3, V(\beta_P)=3, V(\beta_L)=3, V(d_{P_{16,20}})=1, V(d_{P_{17,21}})=1$	95%
$V(\gamma)=2, V(\alpha_P)=2, V(\alpha_L)=2, V(\beta_P)=2, V(\beta_L)=2, V(d_{P_{16,20}})=1, V(d_{P_{17,21}})=1, V(\sigma^2_{P_{6,y}})=1, V(\sigma^2_{P_{20,y}})=1, V(\sigma^2_{P_{16,y}})=1$	66%
$V(\gamma)=5, V(\alpha_P)=5, V(\alpha_L)=5, V(\beta_P)=5, V(\beta_L)=5, V(d_{P_{16,20}})=1, V(d_{P_{17,21}})=1, V(\sigma^2_{P_{6,y}})=1, V(\sigma^2_{P_{20,y}})=1, V(\sigma^2_{P_{16,y}})=1$	80%
$V(d_{P_{16,20}})=1, V(d_{P_{17,21}})=1$	33%
$V(\sigma^2_{P_{6,y}})=1, V(\sigma^2_{P_{20,y}})=1, V(\sigma^2_{P_{16,y}})=1$	57%
$V(d_{P_{16,20}})=1, V(d_{P_{17,21}})=1, V(\sigma^2_{P_{6,y}})=1, V(\sigma^2_{P_{20,y}})=1, V(\sigma^2_{P_{16,y}})=1$	57%
$V(\omega_h)=1, V(\omega_v)=1$	62%
$V(a_{P_1})=1, V(a_{P_{10}})=1, V(a_{P_{14}})=1, V(a_{P_{17}})=1, V(a_{P_{21}})=1,$	57%
$V(a_{P_1})=1$	47%
$V(a_{P_1})=1,\ V(a_{P_6})=1,\ V(a_{P_9})=1,\ V(a_{P_{13}})=1,\ V(a_{P_{21}})=1, V(a_{P_{17}})=1$	71%
$V(\varphi_{\beta_L})=1, V(\varphi_{\beta_P})=1, V(d_{P_{10,14}})=1, V(d_{P_{9,13}})=1, V(d_{P_{16,20}})=1, V(d_{P_{17,21}})=1, V(a_{P_1})=1, V(a_{P_9})=1, V(a_{P_{13}})=1, V(a_{P_{10}})=1, V(a_{P_{14}})=1, V(a_{P_{20}})=1, V(a_{P_{16}})=1, V(a_{P_{21}})=1, V(a_{P_{17}})=1$	62%

In this work, we have described the parameters of the gait, the ways we calculated them and the methods we examined their relevance. Finally, we used these results to validate their accuracy. We came to the conclusion that the unique parameters are ones that are constant in time. They are body proportions such as height, length of arms and legs. All other parameters were behavioral, and it could be somewhat imitated. We found out that the gait hides a unique biometric signature that could help to identify a person.

REFERENCES

ACAR, E., SENST, T., KUHN, A., KELLER, I., THEISEL, H., ALBAYRAK, S., AND SIKORA, T. 2012. Human action recognition using lagrangian descriptors. In *2012 IEEE 14th International Workshop on Multimedia Signal Processing (MMSP)*. 360–365.

ANDRILUKA, M., ROTH, S., AND SCHIELE, B. 2009. Pictorial structures revisited: People detection and articulated pose estimation. In *2009 IEEE Conference on Computer Vision and Pattern Recognition*. 1014–1021.

BARCLAY, C. D., CUTTING, J. E., AND KOZLOWSKI, L. T. 1978. Temporal and spatial factors in gait perception that influence gender recognition. *Perception & Psychophysics 23,* 2, 145–152.

BAZIN, A. I. AND NIXON, M. S. 2005. Gait verification using probabilistic methods. In *Application of Computer Vision, 2005. WACV/MOTIONS '05 Volume 1. Seventh IEEE Workshops on*. Vol. 1. 60–65.

BORG, I. AND GROENEN, P. 2013. *Modern Multidimensional Scaling: Theory and Applications*. Springer Series in Statistics. Springer New York.

CHEN, D., WACTLAR, H., Y. CHEN, M., GAO, C., BHARUCHA, A., AND HAUPTMANN, A. 2008. Recognition of aggressive human behavior using binary local motion descriptors. In *2008 30th Annual International Conference of the IEEE Engineering in Medicine and Biology Society*. 5238–5241.

DUBOIS, A. AND BRESCIANI, J. P. 2015. Person identification from gait analysis with a depth camera at home. In *2015 37th Annual International Conference of the IEEE Engineering in Medicine and Biology Society (EMBC)*. 4999–5002.

ĎURIKOVIČ, R. AND MADARAS, M. 2015. Controllable skeleton-sheets representation via shape diameter function. In *Mathematical Progress in Expressive Image Synthesis II*, H. Ochiai and K. Anjyo, Eds. Springer Japan, Tokyo, 79–90.

FENG, Y., LI, Y., AND LUO, J. 2016. Learning effective gait features using lstm. In *2016 23rd International Conference on Pattern Recognition (ICPR)*. 325–330.

GIANARIA, E., GRANGETTO, M., LUCENTEFORTE, M., AND BALOSSINO, N. 2014. *Human Classification Using Gait Features*. Springer International Publishing, Cham, 16–27.

KIM, J. AND KIM, M. 2014. Motion capture with high-speed rgb-d cameras. In *2014 International Conference on Information and Communication Technology Convergence (ICTC)*. 394–395.

O'HAVER, T. 2016. *A Pragmatic Introduction to Signal Processing: With Applications in Scientific Measurement*. CreateSpace Independent Publishing Platform.

PETERKOVA, A. AND STREMY, M. 2015. Obtaining the gait parameters from kinect sensor for the person identification. In *2015 IEEE 19th International Conference on Intelligent Engineering Systems (INES)*. 337–340.

RAHMAN, M. W. AND GAVRILOVA, M. L. 2017. Kinect gait skeletal joint feature-based person identification. In *2017 IEEE 16th International Conference on Cognitive Informatics Cognitive Computing (ICCI*CC)*. 423–430.

RIEČICKÝ, A., MADARAS, M., PIOVARCI, M., AND DURIKOVIC, R. 2018. Optical-inertial synchronization of mocap suit with single camera setup for reliable position tracking. In *Proceedings of the 13th International Joint Conference on Computer Vision, Imaging and Computer Graphics Theory and Applications - Volume 1: GRAPP,*. INSTICC, SciTePress, 40–47.

TAUTZ, D. 1989. Hypervariability of simple sequences as a general source for polymorphic dna markers. *Nucleic Acids Research 17,* 16, 6463.

TELFORD, W., TELFORD, W., GELDART, L., AND SHERIFF, R. 1990. *Applied Geophysics*. Monograph series. Cambridge University Press.

WANG, Y., LAU, D. L., AND HASSEBROOK, L. G. 2010. Fit-sphere unwrapping and performance analysis of 3d fingerprints. *Appl. Opt. 49,* 4 (Feb), 592–600.

YAM, C., NIXON, M. S., AND CARTER, J. N. 2002. On the relationship of human walking and running: automatic person identification by gait. In *Object recognition supported by user interaction for service robots*. Vol. 1. 287–290 vol.1.

ZHU, L., HU, X., AND KAVAN, L. 2015. Adaptable anatomical models for realistic bone motion reconstruction. *Comput. Graph. Forum 34,* 2 (May), 459–471.

Andrej Mihálik
Mathematics, Physics and Informatics,
Comenius University,
842 48 Bratislava, Slovak Republic
email: andrej.mihalik@fmph.uniba.sk

Roman Ďurikovič
Faculty of Mathematics, Physics and Informatics,
Comenius University,
842 48 Bratislava, Slovak Republic
email: roman.durikovic@fmph.uniba.sk

Michal Sejč
Faculty of Mathematics, Physics and Informatics,
Comenius University,
842 48 Bratislava, Slovak Republic